CVJ CLUJ VETERINARY JOURNAL

Research Article

Correlating Eosin Fluorescence Patterns and Basophilic Alterations in a DEN-Induced HCC Murine Model Through Confocal Microscopy

Romelia Pop [1]*, Dragoș Hodor[1], Cornel Cătoi[1], Teodora Mocan[2,3], Lucian Mocan[2,4] and Alexandru-Flaviu Tăbăran[1]

[1] Department of Pathology, Faculty of Veterinary Medicine, University of Agricultural Sciences and Veterinary Medicine of Cluj-Napoca, Calea Manașstur, 400372 Cluj-Napoca, Romania; romelia.pop@usamvcluj.ro; dragos.hodor@usamvcluj.ro; cornel.catoi@usamvcluj.ro; alexandru.tabaran@usamvcluj.ro;
[2] Nanomedicine Department, Regional Institute of Gastroenterology and Hepatology "Octavian Fodor";
[3] Department of Physiology, University of Medicine and Pharmacy, "Iuliu Hatieganu"; teodora.mocan@umfcluj.ro
[4] 3-rd Surgery Clinic, University of Medicine and Pharmacy, 400162 Cluj-Napoca, Romania; lucian.mocan@umfcluj.ro
*Correspondence: romelia.pop@usamvcluj.ro; Tel: +40744263975

Abstract: Hepatocellular carcinoma is a major global health concern and a leading cause of cancer-related mortality. This study employed chemically induced murine models to simulate human hepatocellular carcinoma, utilizing 28 albino Swiss mice with the administration of a single dose of the complete carcinogen diethylnitrosamine (DEN) at 100mg/kg, followed by serial euthanasia. The focus was on understanding early hepatocellular alterations and distinguishing precursor changes from incidental changes. The assessment of hepatocellular alteration foci relied on hematoxylin and eosin (H&E) staining. However, the research introduced a novel approach by exploiting the fluorescence properties of eosin, a component of the H&E stain. This approach was applied to investigate basophilic alteration foci indicating alterations in cellular composition exhibiting notably heightened RNA staining. To achieve this, confocal laser scanning microscopy was employed, correlating changes in fluorescence intensity with tinctorial alterations. The histological examination revealed that basophilic foci displayed unique nodular lesions with intense basophilic cytoplasm. Nuclear alterations, including hyperchromasia and basophilia, contributed to understanding cellular and nuclear changes in these foci. Statistical analysis highlighted a discernible reduction in eosin fluorescence intensity within basophilic foci compared to normal hepatic tissue.

Keywords: hepatocellular carcinoma; animal model; basophilic foci; histology, eosin, confocal microscopy

1. Introduction

Received: 14 December 2023
Accepted: 15 March 2024
Published: 9 April 2024

DOI:10.52331/nqpej009

Hepatocellular carcinoma (HCC) ranks as the fifth most prevalent neoplasm in humans worldwide and stands as the primary cause of cancer-related mortality in specific regions [1]. This reality drives continuous research directed at formulating innovative therapies and diagnostic methods. The investigation into HCC mechanisms and the assessment of potential treatments heavily rely on animal models. Apart from spontaneous models involving animals like dogs and woodchucks, chemically induced rodent models take a central position in HCC research [2-5]. The administration of the carcinogenic and mutagenic compound Diethylnitrosamine (DEN) (CH3-CH2)2N-N=O) through parenteral or oral routes in experimental models animals is particularly utilized for its significant translational value in understanding the complex profile of aggressive forms of hepatocellular carcinoma (HCC) in humans [6]. DEN-induced hepatic tumors in rodents, through various mechanisms such as epigenetic and genetic changes, typically undergo a sequential progression. This starts with an initial phase of inflammation and necrosis, leading to long-term hepatocellular hyperplastic and dysplastic

changes, defined as "alteration foci," ultimately resulting in neoplastic transformation, including hepatocellular adenoma and carcinoma [7,8]. The hepatocellular "alteration foci" are identified as preneoplastic changes, characterized by their distinctive staining patterns on the conventional hematoxylin and eosin (HE) stain. While both acidophilic and basophilic foci are referenced in the context of hepatocellular alteration, in cases of HCC induced by DEN, the "basophilic foci" emerge as the primary preneoplastic phenotype changes in hepatocytes. Despite being mechanistically complex, the hepatocellular basophilic phenotype observed in alteration foci in DEN-induced HCC is attributed to metabolic shifts within cells. This reflects a progressive transition from anabolic to catabolic glucose metabolism, indicative of the Warburg effect, to sustain irregular cell proliferation [9]. A significant problem in comprehending the progression of chemically induced hepatocellular carcinomas in rodents is distinguishing early hepatocellular alterations that serve as precursors to carcinomas from those that are incidental or secondary phenomena [10]. The conventional method for defining and assessing hepatocellular alteration foci [11] traditionally relies on H&E staining. This classic staining technique, employed in all regulatory toxicological studies in animal models, utilizes hematoxylin ($C_{16}H_{14}O_6$) to stain anionic components (like DNA and RNA). Simultaneously, the xanthene pigment eosin Y ($C_{20}H_6Br_4Na_2O_5$) is applied to stain cationic compounds (such as proteins). Eosin Y binds electrostatically to the carboxylic and phenolic groups of arginine, histidine, lysine, and tryptophan residues [12]. Interestingly, Eosin is produced through the bromination of fluorescein, displaying a fluorescence photoactivity similar to its parent compound [13]. This unique fluorescence characteristic of eosin has been recently utilized as a diagnostic tool for quantifying liver injury [14]. Moreover, eosin serves as a fluorescent pH indicator, and certain derivatives are employed as reactive fluorescent labels. Eosin Y and fluorescein are applied as benchmarks for quantum yield, photosensitizing agents, laser dyes, and labeling biological specimens [15]. The present work aims to systemically assess the changes in the eosin fluorescence pattern in the preneoplastic, basophilic hepatic nodules obtained in a DEN-induced HCC murine model.2. Materials and Methods

Animals

The study involved 28 albino Swiss mice, young males, with an average weight of around 25g. Mice of the Swiss strain were purchased according to the regulations in force from the Iuliu Haţieganu UMF Animal Facilities Cluj-Napoca. These mice were housed in plastic cages with unrestricted access to food and water, under conditions of 22–23°C temperature, 55% humidity, and a 12-hour light/dark cycle. They were provided with standard pelleted rodent feed manufactured by Cantacuzino National Insitute for Medical-Military Research and Development. The research protocol received approval from DSVSA (National Veterinary Medicine Authority no. 267/12.07.2021). All procedures related to the use of laboratory animals adhered to the guidelines and European regulations outlined in EU Directive 2010/63/EU and Romanian law 43/2014.

Experimental design

The procedure for inducing liver carcinoma was modified from the method outlined by Sun et al. in 2012 [16], involving the following steps. The mice were assigned to four groups (Control, G1, G2, and G3), each with seven mice. Before each injection, mice were weighed to ensure accurate calculation of the diethylnitrosamine (DEN) dose. A single intraperitoneal dose of diethylnitrosamine at 100mg/kg was administered. The progression of hepatic alterations and HCC was monitored over time by systematically euthanizing animals at 2 months (G1), 5 months (G2), and 8 months (G3) post-DEN administration. The mice were euthanized with prolonged exposure to isoflurane. The spontaneous

deaths were not recorded during this experiment.The analysis of eosin fluorescence was carried out on the first and second sacrificed groups in which the presence of basophilic foci was observed..

Histopathological analysis

The liver was sampled for subsequent analysis and fixed in 10% formalin for 48 hours. Samples were fixed, dehydrated, and clarified in ethyl alcohol and xylene. Paraffin infiltration at 58°C for 5 hours was done, and 2 μm-thin sections were obtained. For staining, slides underwent xylene immersion, ethanol solutions, hematoxylin, and eosin Y. Dehydration included ethanol immersions, and clearing was done with xylene. Finally, Permount and coverslips were applied for microscopic observation of stained tissue sections. [17]. Histological examination of the samples was conducted using an Olympus BX51 microscope, and bright field images were captured using an Olympus SP350 digital camera, and processed using the Olympus cellSens software. The assessment of liver histopathology was performed based on the International Harmonization of Nomenclature and Diagnostic (INHAND) histological criteria standards for rodents [11.]*Chemical and Reagents*

N-Nitrosodiethylamine solution was purchased from Sigma (Lot# 049K1613). H&E staining kit was acquired from Abcam (H&E Staining Kit ab245880).

Confocal scanning laser microscopy (CSLM) analysis

Confocal fluorescent pictures were captured utilizing a Zeiss LSM 710 confocal laser scanning module installed on an Axio Observer Z1 Inverted Microscope. To visualize cell structures, a 488 excitation laser line was employed to detect Eosine (BP 493-625 nm emission). All pictures were taken with a Plan Apochromat 63× (1.4; oil immersion, DIC M27) Zeiss objective. Standard ZEN software provided by the Zeiss system manufacturer was utilized for image merging, processing, and analysis. Fluorescence values were denoted in arbitrary units (AU).

Eosine quantification by CLSM

The assessment of Eosine expression in the liver followed a methodology similar to our previous work [18]. Quantitative analysis of the confocal images was automated using the point-by-point fluorescence quantification functions within the ZEN software. To ensure consistent quantification conditions and maintain high reproducibility, CLSM image acquisition was standardized and upheld throughout the experiment (acquisition time 30 s, lasers' output power 20%, pinhole diameter 53 μm, master gain 420, digital gain 15 Each image section measured 512 × 512 pixels (135× 135μm), covering an area of 18.225 μm² for every scanned microscopic field. Mean fluorescence was assessed on five basophilic foci by examining two fields (obx63) per focus (totaling 10 fields with basophilic foci). In a similar matter, the perilesional liver for each basophilic focus was assessed in 2 histological fields from the same histological slides. Additionally, measurements on 10 fields from an uninjected mouse serving as the control were conducted *Statistical analysis*

Statistical evaluations were conducted utilizing RStudio version 4.3.1. For datasets distribution it was used the Shapiro-Wilk normality test. To assess the intensity of the Eosine in the Kruskal-Wallis and with Dunn's post-hoc analysis with Bonferroni correction was utilized.

3. Results

Modifications associated with DEN administration were noted in the second and third groups, occurring approximately 5 and 8 months following administration. Pathologically, the first group (sacrificed at 2 months) showed no visible macroscopic changes, while the second group displayed distinct masses in four out of seven examined livers. The masses were white-beige, well-demarcated, measuring up to 3 mm, with a multifocal or multifocal-coalescing arrangement, distributed in all hepatic lobes (up to 15 masses /liver). Similarly, in the third experimental group, masses were detected in five out

of seven examined livers. In this group, the masses measure up to 1 cm, maintaining the same multifocal or multifocal-coalescing arrangement as in group 3. Intratumoral necrosis was occasionally noted in the masses of this group. Histologically, the basophilic foci, (randomly distributed and predominantly observed within the initial two groups and evaluated in the context of this experiment), consist of well-defined, nodular, circular, un-encapsulated lesions characterized by hepatocytes organized in interconnected cord-like structures, exhibiting minimal cellular polymorphism. These foci prominently displayspecific tinctorial staining patterns and granularity. The global tissue architecture within the basophilic foci experiences a moderate level of disruption**.** The cellular components in these foci may appear darker (basophilic) compared to adjacent tissues. The majority of hepatocytes within the basophilic foci exhibit a prominent abundance of granular and intensely basophilic cytoplasm. Noteworthy histological features encompass nuclear alterations, including occasional nuclear enlargement, and heightened chromatic intensity (hyperchromasia). The nuclei within these foci reveal vacuolated chromatin, and in some instances, the presence of 1-2 distinct basophilic nucleoli. These observed histopathological characteristics collectively contribute to the comprehensive understanding of the cellular and nuclear alterations inherent in basophilic following DEN administration (Figure 1 image A, B, C).

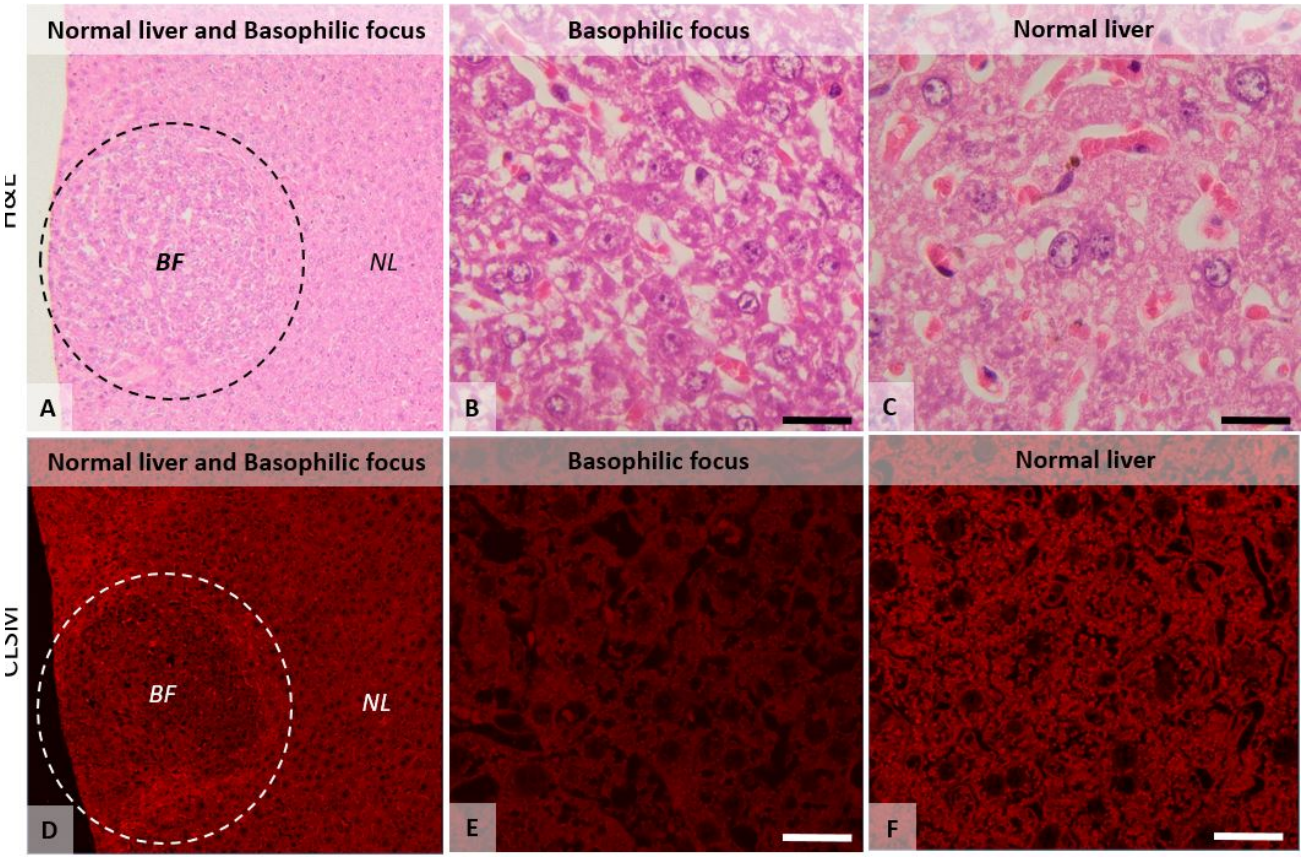

Figure. 1. Histological images (A, B and C) and Confocal laser (D, E, and F) of the mice liver, comparing the hepatocellular preneoplastic basophilic alteration foci (BF) with the normal liver parenchyma (NL). Image A. Histological micrographs showing a well-demarcated, subscapular hepatocellular basophilic focus (BF), characterized by tortuously arranged hepatic chords, with hepatocytes showing increased cytoplasmic basophilia relative to adjacent normal parenchyma, without significant compression of the bordering tissue. Image B. The hepatocytes of the basophilic focus, are

characterized by bands of localized, clumped basophilic bodies in the peripheral cytoplasm with clear intervening areas ("tigroid" pattern). **Image B.** Hepatocytes from the control group, showing normal patterns of cytoplasmic staining. Image D. Confocal images of the basophilic focus (BF) presented in image A, showing reduced overall fluorescence compared with the adjacent hepatic tissue (NL). Image E. Confocal images of the hepatocytes from the basophilic focus, showing a reduced cytoplasmic fluorescence compared with the fluorescence observed in the adjacent, normal liver (image F). CLSM objective 10 (image D) and x63×/1.4 Oil Plan Apochromatic objective (images E and F); H&E images, ob x10 (images A) and x 100 (images B and C). Scale bar=20μm.

Concerning the CLSM manifestation of Eosin expression, a discernible reduction in fluorescence intensity was evident when comparing normal hepatic tissue to basophilic foci. Within the confines of a morphological normal liver, the fluorescence intensity of Eosin exhibits a visibly elevated profile as opposed to the diminished Eosin fluorescence encountered within basophilic foci, thereby indicating a discernible alteration in Eosin fluorescence within the latter. (Figures 1 Image D,E,F, and Figure 2,).

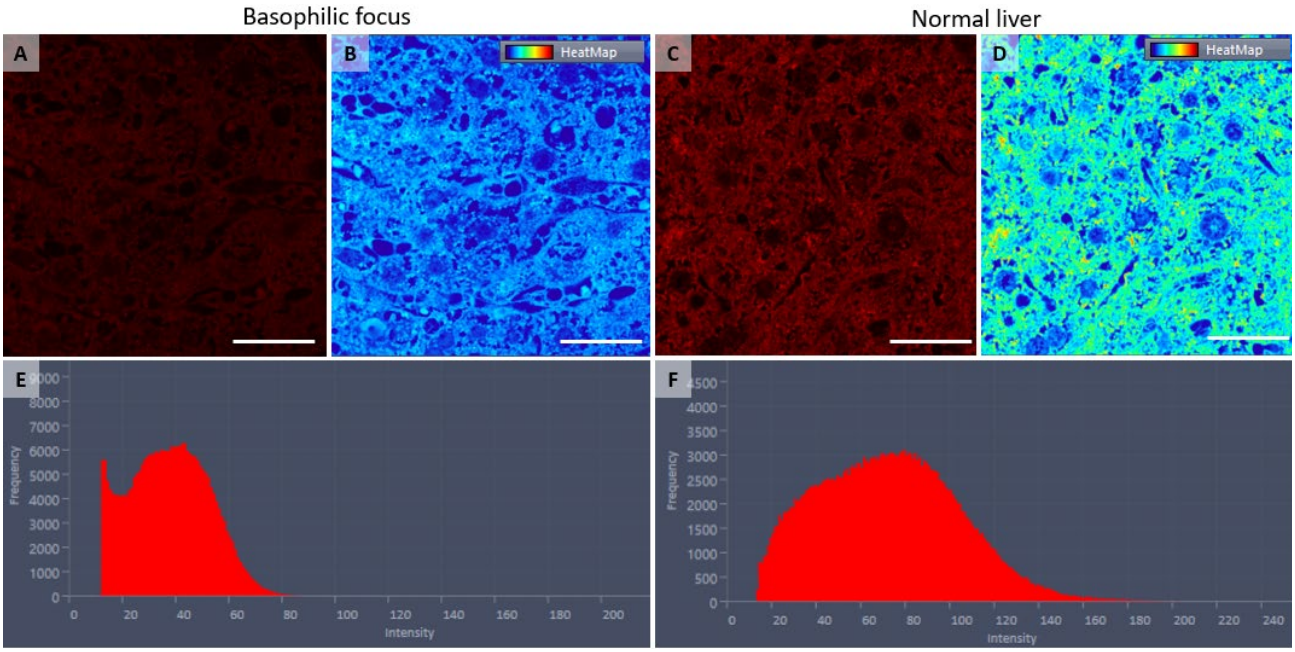

Figure. 2. Confocal laser scanning microscopy micrographs of liver tissue, presenting the basophilic foci (images A and B) and their fluorescence spectra (image E) compared with the normal adjacent liver parenchyma (images C, and D) and its fluorescent spectra (image F). The fluorescence intensity distribution histograms (images E and F) show the altered expression of the Eosin/fluorescein within the hepatocytes of the basophilic foci compared with normal hepatic tissue. The Eosin/fluorescein expression = red channel. Images B and D compare the fluorescence expression of Eosin/fluorescein as a heatmap in the basophilic foci (B) compared with normal tissue hepatic (D). Warmer colors indicate higher Eosin/fluorescein expression intensities. 63×/1.4 Oil Plan Apochromate objective.

Statistically, the Shapiro-Wilk test indicates that the data for all groups are normally distributed. Posthoc Dunn's test with Bonferroni correction revealed significant differences between the "Basophilic foci" group and both the "Normal liver (control)" and "Normal liver (perilesional)" groups, but not between the latter two. Specifically, the comparison of basophilic foci with normal liver (control) yielded a P-value of 0.00485, while the comparison with normal liver (perilesional) also resulted in a P-value of 0.00485. Despite the data's normality, the Kruskal-Wallis test revealed significant differences among the groups' medians, with post-hoc Dunn's test confirming significant disparities between the "Basophilic foci" group and both "Normal liver (control)" and "Normal liver (perilesional)" groups, albeit not between the latter two.

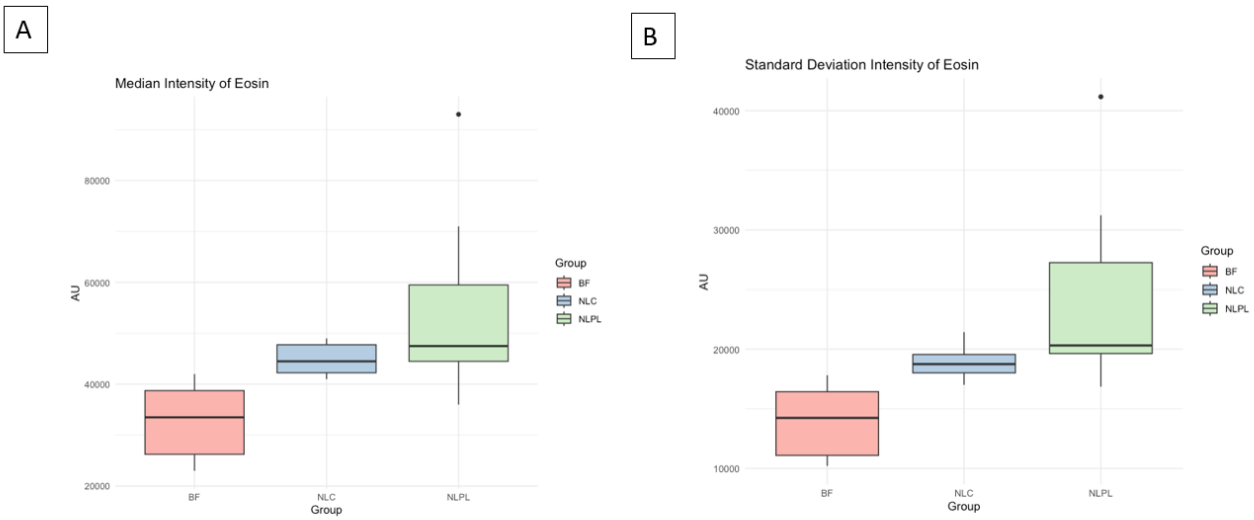

Figure 3. Image A. represets Comparative Analysis of Eosin Median Intensity Across Liver Tissue Conditions in Mice. Box plot A representation of the median intensity of eosin staining across three distinct liver tissue conditions in mice: Basophilic foci (BF), Normal liver (control, NLC), and Normal liver (perilesional, NLPL). The eosin median intensity is markedly lower in Basophilic foci (BF) compared to Normal liver (control, NLC), suggesting a diminished central tendency of eosin intensity in BF. In contrast, the median intensity in Normal liver (perilesional, NLPL) is elevated, indicating a higher eosin affinity or increased density of staining in perilesional compared to control tissues. These observations may reflect differential eosinophilic activity or structural variations among the hepatic conditions examined. Image B represents Variability in Eosin Staining Intensity Among Liver Tissue Conditions in Mice. This box plot illustrates the variability, as measured by standard deviation, of eosin staining intensity within three different liver tissue conditions in mice: Basophilic foci (BF), Normal liver (control, NLC), and Normal liver (perilesional, NLPL). The standard deviation is substantially lower in the Basophilic foci (BF) group, suggesting more homogeneity in staining intensity, whereas the Normal liver (perilesional, NLPL) exhibits a higher standard deviation, indicating greater variability in eosin uptake or distribution. The Normal liver (control, NLC) shows intermediate variability. These differences in standard deviation may imply distinct histological characteristics or differential responses to staining due to the underlying pathology of the tissue."

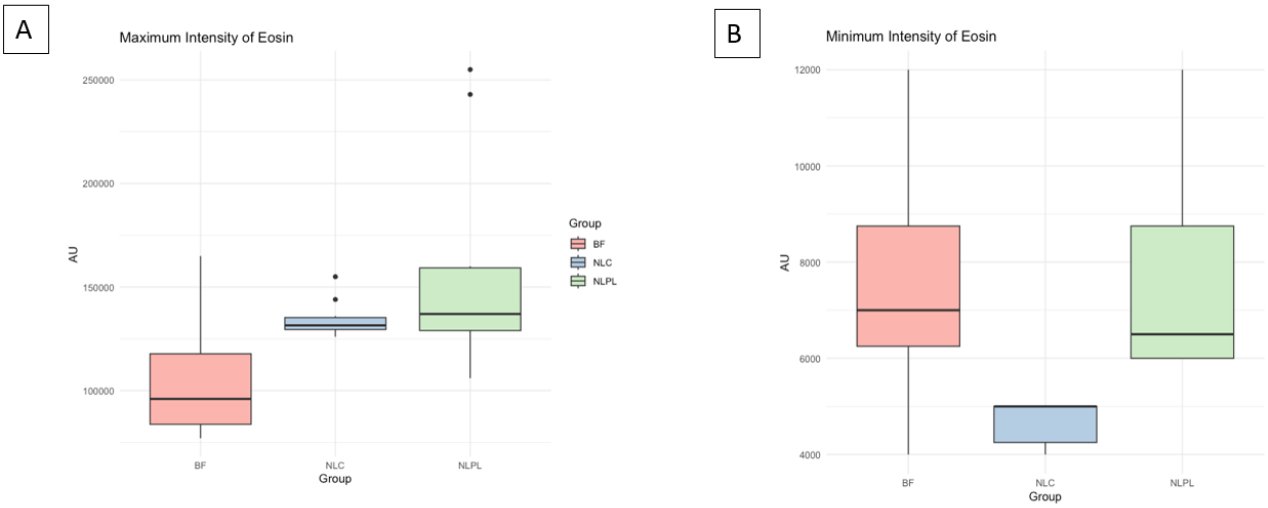

Figure 4. Image A represents Evaluation of Maximum Eosin Staining Intensity in Diverse Liver Tissue States in Mice. The box plot showcases the maximum intensity of eosin staining within three liver tissue states: Basophilic foci (BF), Normal liver (control, NLC), and Normal liver (perilesional, NLPL). The Basophilic foci (BF) group exhibits a lower range of maximum intensity, suggesting a restricted eosin presence or a lesser degree of staining peak. In contrast, the Normal liver (perilesional, NLPL) displays a substantially higher maximum intensity, indicating intense eosinophilic engagement or staining concentration, potentially reflective of heightened inflammatory or morphological alterations in perilesional tissue**.** Image B represents Assessment of Minimum Eosin Staining Intensity Across Varied Liver Conditions in Mice. The box plot depicts the minimum intensity of eosin staining for Basophilic foci (BF), Normal liver (control, NLC), and Normal liver (perilesional, NLPL) conditions in murine hepatic tissue. The minimum intensity levels are notably higher in the Basophilic foci (BF) and Normal liver (perilesional, NLPL) groups compared to the Normal liver (control, NLC), indicating a greater baseline level of eosin staining in these conditions. This could suggest a floor effect of eosinophil infiltration or binding affinity in the BF and NLPL tissues."

4. Discussion

In rodent toxicity experiments involving specific xenobiotics, cellular changes known as basophilic foci are observable alterations in liver tissue. These changes, visible under stains like H&E, reveal unique characteristics in terms of cell type, staining patterns, and texture, offering insights into liver morphological variations linked to hepatocarcinogenesis [19]. Basophilic foci typically appear as circular or ovoid lesions, differing noticeably from normal liver tissue in staining reactions and cellular appearance. The differentiation of basophilic foci types, based on staining attributes, hepatocyte size, and texture, aids in understanding the complex cellular transformations within the liver. While maintaining lobular architecture, these foci may vary in portal areas and central veins depending on their size. Compression of sinusoids within the foci can affect the detection of typical parenchymal plates, and increased cellular numbers may lead to the development of tortuous hepatic cords [11].

Early stages of hepatocarcinogenesis induced by DEN administration involve molecular changes highlighted by Watanabe et al. [20], revealing mRNA networks associated with cancer-related genes, cell cycle regulation, and cell death. The progression from pre-neoplastic foci to distinct phenotypes such as basophilic, eosinophilic, or clear cell foci is linked to metabolic turnover, with specific molecular events driving this transition. Elevated insulin growth factor 2 (IGF-2) levels and downstream signaling play key roles in shaping glycogen storage phenotypes, ultimately leading to the basophilic phenotype [21]. Initially, exposure to DEN elevates insulin IGF-2 levels, initiating downstream signaling that reduces glucose-6-phosphatase (G6Pase) activity, resulting in glycogen storage phenotypes. Moreover, IGF signaling activates the Ras/Raf mitogen-activated signaling cascade, promoting cell proliferation [22]. Over time, the foci transition from anabolic to catabolic glucose metabolism to support cell proliferation, culminating in the development of the basophilic phenotype. Some altered hepatocyte foci (AHF) exhibit mutations in Hras and Braf oncogenes, potentially providing a growth advantage, as these molecular alterations are more frequently observed in late-stage neoplastic lesions [23]. Braf mutations induce ERK1/Akt hyperphosphorylation, leading to the induction of pro-survival/pro-proliferative complement component C5/C5a in basophilic foci [24]. Consequently, AHF are generally considered putative preneoplastic lesions in chemically induced models, although the full significance of morphologically similar lesions in human hepatocarcinogenesis remains incompletely understood.

The development of hepatocellular carcinoma (HCC), involving initiation, promotion, and progression, is influenced by interactions among genetic, epigenetic, and environmental factors. Initiation often arises from genetic mutations induced by various carcinogens, such as aflatoxin, hepatitis B or C viruses, alcohol, metabolic disorders, and inflammation, causing DNA damage [26,27]. Chronic liver diseases create a conducive environment for HCC promotion, leading to the accumulation of genetic abnormalities and preferential selection of growth-advantaged cells. Subsequent genetic modifications in the promotion phase activate oncogenes, facilitate cell growth, and deactivate tumor suppressor genes, collectively contributing to unregulated cell multiplication [28,29]. As tumors progress, angiogenesis is triggered for continued growth, enabling infiltration into adjacent tissues and dissemination to distant organs, involving alterations in adhesion, migration, and invasion. HCC strategically evades the immune system, avoiding detection and elimination by the body's innate defense mechanisms [30,31].

Traditional staining methods, like hematoxylin-eosin, and selective fluorescence reactions, notably with eosin Y, provide valuable tools for histological examination. Eosin Y's versatility extends beyond histology, serving as a fluorescent dye for various cellular structures, highlighting its utility in diverse applications [13,32]. By comparing optical images of basophilic alteration foci stained by H&E with their confocal fluorescence spectra, a correlation between the loss of fluorescence intensity and loss of hepatocyte tinctorial affinity for eosin (defined as "basophilia") is observed. These findings are significant from a diagnostic perspective, employing confocal laser scanning microscopy (CLSM) as a tool in toxicological pathology, aiding in establishing the link between tinctorial changes of basophilic foci (preneoplastic changes) and their fluorescence spectral shifts

5. Conclusions

Following this study, we managed to demonstrate the presence of alterations in the fluorescence spectrum of eosin when bound to proteins in both normal and tumoral liver tissues. This highlights how fluorescence spectroscopy can potentially complement histopathological observations and unveil information that aligns with classical H&E staining methods. Given its inherent

sensitivity to changes in the biomolecular composition across diverse cell and tissue types, fluorescence microscopy can offer information surpassing that of individual conventional diagnostic techniques. Anticipating widespread applications, we envision that this fluorescence imaging approach will prove valuable in diverse fields, including cell biology, biomedical analysis and diagnosis, and the chemical identification of various components within cells and tissues.

Author Contributions: RP, AFT, and TM carried out the HCC protocol. RP and AFT carried out the histological and CLSM assessment and drafted and reviewed the manuscript. DH was involved in the data analysis and statistics. CC and LM reviewed the manuscript. All authors read and approved the final manuscript.

Funding: The authors wish to acknowledge funding granted by the National Authority for Scientific Research and Innovation Romania, CNCS-UEFISCDI, cod PN-III-P2-2.1-PED-2021-0073 and PN-III-P2-2.1-PED-2019-0997.

Institutional Review Board Statement: The experimental protocol has been approved by DSVSA (National Veterinary Medicine Authority no. 267/12.07.2021). All procedures involving the use of laboratory animals followed the guidelines and European norms 337 established by EU Directive 2010/63/EU and Romanian law 43/2014

Data Availability Statement: The data that support the findings of this study are available from the Department of Veterinary Pathology, University of Agriculture Science and Veterinary Medicine. Data are, however available from the authors upon reasonable request and with the permission of the Department of Veterinary Pathology, University of Agriculture Science and Veterinary Medicine.

Acknowledgments: Not applicable

Conflicts of Interest: The authors declare no conflict of interest.

References

1. Bruix, Jordi, Loreto Boix, Margarita Sala, and Josep M. Llovet. "Focus on hepatocellular carcinoma." Cancer cell 5, no. 3 (2004): 215-219.
2. Zhang, Hui Emma, James M. Henderson, and Mark D. Gorrell. "Animal models for hepatocellular carcinoma." Biochimica et Biophysica Acta (BBA)-Molecular Basis of Disease 1865, no. 5 (2019): 993-1002.
3. Li, Yan, Zhao-You Tang, and Jin-Xuan Hou. "Hepatocellular carcinoma: insight from animal models." Nature reviews Gastroenterology & hepatology 9, no. 1 (2012): 32-43.
4. Li, Enya, Li Lin, Chia-Wei Chen, and Da-Liang Ou. "Mouse models for immunotherapy in hepatocellular carcinoma." Cancers 11, no. 11 (2019): 1800.
5. Suresh, Manasa, and Stephan Menne. "Application of the woodchuck animal model for the treatment of hepatitis B virus-induced liver cancer." World Journal of Gastrointestinal Oncology 13, no. 6 (2021): 509.
6. Romualdo, Guilherme Ribeiro, Kaat Leroy, Cícero Júlio Silva Costa, Gabriel Bacil Prata, Bart Vanderborght, Tereza Cristina Da Silva, Luís Fernando Barbisan et al. "In vivo and in vitro models of hepatocellular carcinoma: current strategies for translational modeling." Cancers 13, no. 21 (2021): 5583.
7. Uehara, Takeki, Igor P. Pogribny, and Ivan Rusyn. "The DEN and CCl4-induced mouse model of fibrosis and inflammation-associated hepatocellular carcinoma." Current protocols in pharmacology 66, no. 1 (2014): 14-30.
8. Kurma, Keerthi, Olivier Manches, Florent Chuffart, Nathalie Sturm, Khaldoun Gharzeddine, Jianhui Zhang, Marion Mercey-Ressejac et al. "DEN-induced rat model reproduces key features of human hepatocellular carcinoma." Cancers 13, no. 19 (2021): 4981.
9. Suzuki, Hideo, Motoyuki Kohjima, Masatake Tanaka, Takeshi Goya, Shinji Itoh, Tomoharu Yoshizumi, Masaki Mori et al. "Metabolic alteration in hepatocellular carcinoma: mechanism of lipid accumulation in well-differentiated hepatocellular carcinoma." Canadian Journal of Gastroenterology and Hepatology 2021 (2021): 1-13.
10. Goldfarb, Stanley, Thomas D. Pugh, Hirofumi Koen, and Yu-Zhu He. "Preneoplastic and neoplastic progression during hepatocarcinogenesis in mice injected with diethylnitrosamine in infancy." Environmental Health Perspectives 50 (1983): 149-161.
11. Thoolen, Bob, Robert R. Maronpot, Takanori Harada, Abraham Nyska, Colin Rousseaux, Thomas Nolte, David E. Malarkey et al. "Proliferative and nonproliferative lesions of the rat and mouse hepatobiliary system." Toxicologic pathology 38, no. 7_suppl (2010): 5S-81S.
12. Chan, John KC. "The wonderful colors of the hematoxylin–eosin stain in diagnostic surgical pathology." International journal of surgical pathology 22, no. 1 (2014): 12-32

13. Acharya, Seema, and Babulal Rebery. "Fluorescence spectrometric study of eosin yellow dye–surfactant interactions." Arabian Journal of Chemistry 2, no. 1 (2009): 7-12.
14. Ali, Hamid, Safdar Ali, Maryam Mazhar, Amjad Ali, Azra Jahan, and Abid Ali. "Eosin fluorescence: A diagnostic tool for quantification of liver injury." Photodiagnosis and Photodynamic Therapy 19 (2017): 37-44.
15. De Rossi, Andiara, Lenaldo B. Rocha, and Marcos A. Rossi. "Application of fluorescence microscopy on hematoxylin and eosin-stained sections of healthy and diseased teeth and supporting structures." Journal of oral pathology & medicine 36, no. 6 (2007): 377-381.
16. Sun, Hua, Linghong Yu, Huailing Wei, and Gengtao Liu. "A novel antihepatitis drug, bicyclol, prevents liver carcinogenesis in diethylnitrosamine-initiated and phenobarbital-promoted mice tumor model." Journal of Biomedicine and Biotechnology 2012 (2012).
17. Cardiff, Robert D., Claramae H. Miller, and Robert J. Munn. "Manual hematoxylin and eosin staining of mouse tissue sections." Cold Spring Harbor Protocols 2014, no. 6 (2014): pdb-prot073411
18. Clichici, Simona, Alexandru Radu Biris, Flaviu Tabaran, and Adriana Filip. "Transient oxidative stress and inflammation after intraperitoneal administration of multiwalled carbon nanotubes functionalized with single strand DNA in rats." Toxicology and Applied Pharmacology 259, no. 3 (2012): 281-292.
19. Harada, Takanori, Robert R. Maronpot, Gary A. Boorman, Richard W. Morris, and Katherine A. Stitzel. "Foci of cellular alteration in the rat liver: a review." Journal of Toxicologic Pathology 3, no. 2 (1990): 161-188.
20. Watanabe, Takashi, Gotaro Tanaka, Shuichi Hamada, Chiaki Namiki, Takayoshi Suzuki, Madoka Nakajima, and Chie Furihata. "Dose-dependent alterations in gene expression in mouse liver induced by diethylnitrosamine and ethylnitrosourea and determined by quantitative real-time PCR." Mutation Research/Genetic Toxicology and Environmental Mutagenesis 673, no. 1 (2009): 9-20.
21. Lahm, Harald, Katinka Gittner, Ottheinz Krebs, Lisa Sprague, Erhard Deml, Doris Oesterle, Andreas Hoeflich, Rüdiger Wanke, and Eckhard Wolf. "Diethylnitrosamine induces long-lasting re-expression of insulin-like growth factor II during early stages of liver carcinogenesis in mice." Growth hormone & IGF research 12, no. 1 (2002): 69-79.
22. Buchmann, Albrecht, Züleyha Karcier, Benjamin Schmid, Julia Strathmann, and Michael Schwarz. "Differential selection for B-raf and Ha-ras mutated liver tumors in mice with high and low susceptibility to hepatocarcinogenesis." Mutation Research/Fundamental and Molecular Mechanisms of Mutagenesis 638, no. 1-2 (2008): 66-74
23. Connor, Frances, Tim F. Rayner, Sarah J. Aitken, Christine Feig, Margus Lukk, Javier Santoyo-Lopez, and Duncan T. Odom. "Mutational landscape of a chemically-induced mouse model of liver cancer." Journal of hepatology 69, no. 4 (2018): 840-850.
24. Parekh, Palak, and K. V. K. Rao. "Overexpression of cyclin D1 is associated with elevated levels of MAP kinases, Akt and Pak1 during diethylnitrosamine-induced progressive liver carcinogenesis." Cell biology international 31, no. 1 (2007): 35-43.
25. Dragan, Y. P., L. Sargent, Y-D. Xu, Y-H. Xu, and H. C. Pitot. "The initiation-promotion-progression model of rat hepatocarcinogenesis." Proceedings of the Society for Experimental Biology and Medicine 202, no. 1 (1993): 16-24.
26. Severi, Tamara, Hannah Van Malenstein, Chris Verslype, and Jos F. Van Pelt. "Tumor initiation and progression in hepatocellular carcinoma: risk factors, classification, and therapeutic targets." Acta Pharmacologica Sinica 31, no. 11 (2010): 1409-1420.
27. Pitot, Henry C., and Alphonse E. Sirica. "The stages of initiation and promotion in hepatocarcinogenesis." Biochimica et Biophysica Acta (BBA)-Reviews on Cancer 605, no. 2 (1980): 191-215.
28. Dapito, Dianne H., Ali Mencin, Geum-Youn Gwak, Jean-Philippe Pradere, Myoung-Kuk Jang, Ingmar Mederacke, Jorge M. Caviglia et al. "Promotion of hepatocellular carcinoma by the intestinal microbiota and TLR4." Cancer cell 21, no. 4 (2012): 504-516.
29. Domínguez-Malagón, Hugo, and Silvia Gaytan-Graham. "Hepatocellular carcinoma: an update." Ultrastructural pathology 25, no. 6 (2001): 497-516.
30. Ogunwobi, Olorunseun O., Trisheena Harricharran, Jeannette Huaman, Anna Galuza, Oluwatoyin Odumuwagun, Yin Tan, Grace X. Ma, and Minhhuyen T. Nguyen. "Mechanisms of hepatocellular carcinoma progression." World journal of gastroenterology 25, no. 19 (2019): 2279.
31. Singh, Amit Kumar, Ramesh Kumar, and Abhay K. Pandey. "Hepatocellular carcinoma: causes, mechanism of progression and biomarkers." Current chemical genomics and translational medicine 12 (2018): 9.
32. Herculano, L. S., L. C. Malacarne, V. S. Zanuto, G. V. B. Lukasievicz, O. A. Capeloto, and N. G. C. Astrath. "Investigation of the photobleaching process of eosin Y in aqueous solution by thermal lens spectroscopy." The Journal of Physical Chemistry B 117, no. 6 (2013): 1932-1937.